*Rom J Morphol Embryol* 2022, 63(1):221–228 ISSN (print) 1220–0522, ISSN (online) 2066–8279 doi: 10.47162/RJME.63.1.25

CASE REPORT

RJME Romanian Journal of Morphology & Embryology http://www.rjme.ro/

# Basaloid squamous cell carcinoma with prominent shadow (ghost) cell differentiation. An unreported neoplasm of the parotid gland

JOSÉ-FERNANDO VAL-BERNAL[1)], GONZALO HERRERA[2)], ALEJANDRO FERNÁNDEZ-FLÓREZ[3)], MARÍA MARTINO[4)]

[1)]*Pathology Unit, Department of Medical and Surgical Sciences, University of Cantabria–IDIVAL, Santander, Spain*

[2)]*Service of Maxillofacial Surgery, Marqués de Valdecilla University Hospital–IDIVAL, Santander, Spain*

[3)]*Service of Radiodiagnosis, Marqués de Valdecilla University Hospital–IDIVAL, Santander, Spain*

[4)]*Service of Anatomical Pathology, Marqués de Valdecilla University Hospital–IDIVAL, Santander, Spain*

## Abstract

Basaloid squamous cell carcinoma (BSCC) is an aggressive type of squamous cell carcinoma (SCC) predominant in the upper aerodigestive tract. To our knowledge, only one case of that tumor has been previously described in the parotid gland. Shadow (ghost) cell differentiation (SCD) is a specialized form of keratinization characteristic of pilomatricoma, and other skin tumors with follicular differentiation. SCD has also been described infrequently in some visceral carcinomas and rarely in the minor salivary glands. Recently, an SCC with prominent SCD has been reported in the parotid. We report for the first time the case of parotid BSCC with prominent SCD in an 87-year-old man. He was admitted due to the appearance in the last few months of a mass, painful on palpation, in the left parotid region. Imaging studies and tru-cut biopsies indicated the need for surgical removal. A left superficial parotidectomy, including the branch of the cervicofacial nerve, was performed. The BSCC showed predominance (62%) of SCD. Immunohistochemically, the basaloid cells were positive for β-catenin, pan-cytokeratin (pan-CK) AE1/AE3, CK19, high-molecular-weight CK (HMWCK), p63, p40, and cluster of differentiation 10 (CD10) in a diffuse pattern. No signs of recurrence or metastasis were observed four months after surgery. The main differential diagnoses include nuclear protein in testis (NUT) carcinoma, adamantinoma-like Ewing sarcoma, embryonal carcinoma, and basal cell adenocarcinoma of the solid type. SCD in BSCC of the parotid should be recognized to avoid misdiagnosis, especially in small samples. Although rare, BSCC with SCD should be added to the list of tumors that may originate in the parotid gland.

***Keywords***: basaloid squamous cell carcinoma, β-catenin, shadow cell differentiation, ghost cell differentiation, salivary gland, parotid.

## Introduction

Basaloid squamous cell carcinoma (BSCC) is an uncommon and aggressive variant of squamous cell carcinoma (SCC) characterized by nests of small cells with a high nuclear to cytoplasmic ratio and scant barely visible cytoplasm and a minor component of conventional SCC. The tumor has a predilection for the upper aerodigestive tract [1–4]. BSCC rarely involves the parotid gland. In fact, to our knowledge, only one case of this neoplasm has been previously reported in that location [5].

So-called shadow (ghost) cells have been regarded as a form of keratinization different from epidermal keratinization and trichilemmal keratinization based on the nuclear accumulation of β-catenin, and deoxyribonucleic acid (DNA) double-strand breaks in precursor cells [6]. Shadow (ghost) cells are cornified cells in which karyolysis occurs with faded nuclei, but the empty nuclear space is still recognizable. These cells show distinct borders, the cytoplasm is ovoid or polyhedral, eosinophilic, filamentous, or granular. Shadow (ghost) cell nests are typically found in pilomatricoma and other cutaneous tumors with follicular differentiation [7–10]. However, shadow (ghost) cells are also observed in noncutaneous tumors, such as calcifying odontogenic cyst (COC) [9], dentinogenic ghost cell tumor (DGCT) [11], ghost cell odontogenic carcinoma (GCOC) [12], adamantinomatous craniopharyngioma [9, 13], gonadal teratomas [14, 15], and some visceral carcinomas [16–30].

Regarding the salivary glands, SCD has rarely been reported in minor salivary gland tumors, mostly as a lesser focal differentiation [31, 32] except for the case reported by Ihrler *et al.* that displayed abundant shadow (ghost) cells [33]. Nevertheless, Harada *et al.* [34] recently documented an exceptional, single case of SCC in the parotid with prominent SCD.

As far as we are aware, BSCC with SCD has not been previously reported in the parotid gland.

### Aim

We herein report the clinical, radiological, pathological, and immunohistochemical (IHC) features of a rare single case of BSCC of the parotid with predominant SCD. In addition, we extensively discuss the general characteristics and diagnostic problems of this unique tumor.

## Case presentation

An 87-year-old, nonsmoker, and nondrinker man was

under follow-up in Dermatology Service for presenting multiple actinic lesions and tumors on the face, scalp, ears, and neck since 1993. In February 2021, he was admitted due to the appearance in the last few months of a 3 cm mass, painful on palpation, in the left parotid region.

His past medical history included successive diagnoses of multiple basal cell carcinomas (BCCs) of the face, neck, and pinna, multiple SCCs of the face, one of them of the spindle cell type, infiltrating porocarcinoma of the right temporal region, atypical fibroxanthoma of the vertex, and various seborrheic keratoses of the face, all of them surgically treated with free surgical margins. The right temporal infiltrating porocarcinoma and left preauricular grade 3 SCC were additionally treated with radiotherapy.

The computed tomography (CT) scan revealed an intraglandular mass of the left parotid space located in the lower part ("tail") of the gland. The mass ventrally contacted the intraglandular vein (a tributary of the internal jugular vein) and dorsally with the anterior surface of the sternocleidomastoid muscle. It was a solid, hyperdense tumor with relatively homogeneous enhancement, peripheral hyperdensity, and a slightly lobulated margin (Figure 1, A and B).

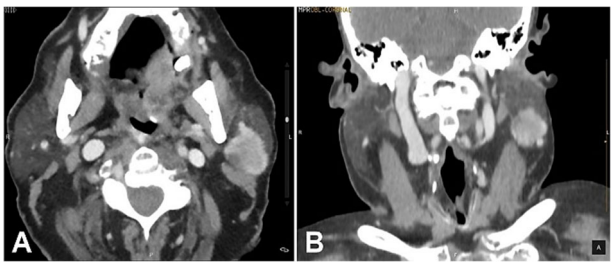


**Figure 1 –** ***CT with contrast-enhanced images: (A) Axial image; (B) Coronal image. Both of them show a hyperdense solid mass with a slight lobulated margin. CT: Computed tomography.***

An ultrasound study revealed an inhomogeneous solid hypoechoic mass with tiny cystic foci, lobulated margin, and irregular borders measuring 3×2.8×2.2 cm located on the tail of the left parotid gland (Figure 2A). Tru-cut biopsies disclosed nests of basaloid cells interspersed with shadow (ghost) cells (Figure 2B). Areas with abundant shadow (ghost) cells were prominent (Figure 2C). These areas comprised 65% of the sampling.

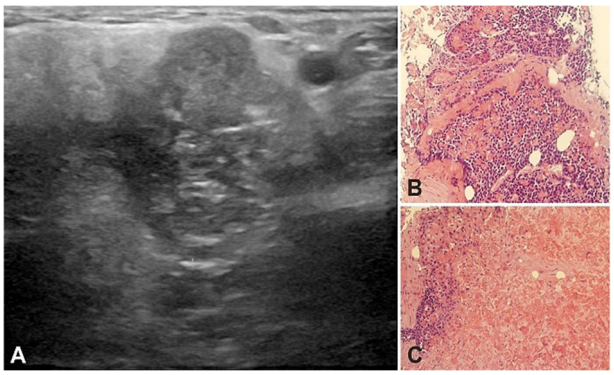


**Figure 2 –** ***US and tru-cut biopsies: (A) Mode B US showing an inhomogeneous solid hypoechoic mass with tiny cystic foci and lobulated margin; (B) Basaloid neoplasia – basaloid cells are interspersed with shadow (ghost) cells; (C) Area with abundant shadow (ghost) cells. HE staining: (B and C) ×200. HE: Hematoxylin–Eosin; US: Ultrasonography.***

On May 19, 2021, a left superficial parotidectomy, including the neoplasm and fibers of the sternocleidomastoid muscle was performed. The branch of the cervicofacial nerve encompassed within the neoplasm was removed. No complications were observed after the intervention.

In the same surgical session, the following lesions were removed: a left preauricular pustular area and seborrheic keratosis, a right preauricular BCC, and a left cervical seborrheic keratosis. Three months later, a SCC was removed from the lobe of the right ear.

The patient remained well, without tumor recurrence, four months after parotidectomy.

## Histopathological findings

The surgical specimen included a segment of parotid and muscle that measured 8×4.2×4 cm of maximum diameters. The macroscopic study revealed a solid, firm, grayish-white, unencapsulated, poorly delimited mass measuring 4.5×4 cm (Figure 3).

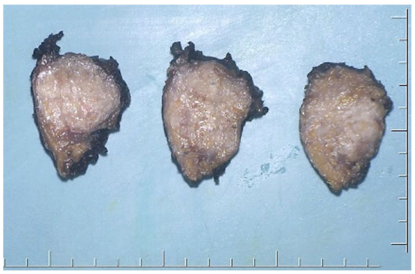

**Figure 3 –** ***The gross specimen shows an ill-defined, grayish-white, solid mass on the cut surface. The parotid reveals adipose infiltration.***

The neoplasm showed no continuity with the skin. The entire surgical specimen was fixed in 10% neutral buffered formalin. Representative tissue samples were embedded in paraffin. For routine microscopy, 5-µm-thick sections were stained with Hematoxylin–Eosin (HE). IHC staining was performed using the EnVision FLEX+ Visualization System (Dako, Agilent Technologies, SL, Las Rozas, Madrid, Spain). The IHC reaction was performed using appropriate tissue controls for the antibodies utilized. Automatic staining was accomplished on a Dako Omnis stainer (Agilent Technologies, SL). The antibodies used are detailed in Table 1.

**Table 1 –** ***IHC antibodies used in this study***

| Antibody | Source | Clone | Dilution | Retrieval solution pH (Dako) |
|---|---|---|---|---|
| α-SMA | Dako | 1A4 | FLEX RTU | High |
| β-Catenin | Dako | β-Catenin-1 | FLEX RTU | *High* |
| SOX10 | Biocare Medical | BC34 | 1:100 | High |
| Pan-CK AE1/AE3 | Dako | AE1/AE3 | FLEX RTU | High |
| CK19 | Dako | RCK108 | FLEX RTU | High |
| HMWCK | Dako | 34βE12 | FLEX RTU | High |
| p63 | Dako | DAK-p63 | FLEX RTU | High |
| p40 | Gennova | BC28 | 1:100 | High |
| CD10 | Dako | 56C6 | FLEX RTU | Low |
| S100 protein | Abcam | Ab55787 | 1:100 | High |

| Antibody | Source | Clone | Dilution | Retrieval solution pH (Dako) |
|---|---|---|---|---|
| CD34 | Dako | QBend 10 | FLEX RTU | High |
| CD56 | Dako | 123C3 | FLEX RTU | High |
| CD57 | Dako | TB01 | FLEX RTU | High |
| CD99 | Dako | 12E7 | FLEX RTU | High |
| CD117 | Dako | Polyclonal | 1:200 | High |
| Calponin | Dako | CALP | 1:200 | High |
| NUT | Dako | C52B1 | 1:50 | High |
| DOG1 (ANO1) | Leica Biosystems | K9 | 1:100 | High |
| CgA | Dako | DAK-A3 | FLEX RTU | High |
| Syn | Dako | SY38 | FLEX RTU | High |
| NSE | Dako | BBS/NC/ VI-H14 | FLEX RTU | High |
| EMA | Dako | E29 | FLEX RTU | High |
| Ki67 | Dako | MIB-1 | FLEX RTU | Low |

α-SMA: Alpha-smooth muscle actin; Abcam, Cambridge, UK; Biocare Medical, SL, Alcalá de Henares, Madrid, Spain; ANO1: Anoctamin 1; CD: Cluster of differentiation; CgA: Chromogranin A; CK: Cytokeratin; Dako (Agilent Technologies, SL, Las Rozas, Madrid, Spain); DOG1: Discovered on gastrointestinal stromal tumor (GIST) 1; EMA: Epithelial membrane antigen; Gennova Scientific, SL, San José de la Rinconada, Sevilla, Spain; HMWCK: High molecular weight cytokeratin; IHC: Immunohistochemical; Leica Biosystems, Barcelona, Spain; NSE: Neuron-specific enolase; NUT: Nuclear protein in testis; RTU: Ready-to-use; SOX10: SRY-box transcription factor 10; Syn: Synaptophysin.

Microscopically, the tumor displayed features of high-grade BSCC with focal keratinization and SCD. It was composed of large, solid lobules, nests, islets, and cords of basaloid cells (Figure 4, A and B). The larger cell clusters were rounded with smooth or sinuous edges. Basaloid cells had a high nuclear to cytoplasmic ratio, dense hyperchromatic nuclei, and little visible cytoplasm. Often the nuclei showed one or more visible nucleoli (Figure 5A). Cells at the edge of the clusters were cuboidal forming complete or incomplete palisades (Figure 5B). Most cell clusters contained abundant keratinized shadow (ghost) cells occupying the middle and central portions. The shadow (ghost) cells made up about 62% of the neoplasm. The transition between shadow (ghost) and basaloid cells was abrupt. Larger nests often exhibited central comedonecrosis (Figure 6A) or sporadic single-cell necrosis (Figure 6B). An extensive basaloid area presented increased nuclear size, with prominent nucleoli, marked pleomorphism, and frequent mitoses (Figure 7A). Occasional foci of definite squamous differentiation expressed by cells with more abundant eosinophilic cytoplasm, intercellular bridges, cells arranged in a paving (mosaic) pattern, or keratin pearl formation were observed (Figure 7B). The squamous differentiation was present isolated or within the nests of the basaloid component and was a minor element of the tumor. There was no transition between the basaloid cells in the nests and the squamous cells. In the peripheral area, the neoplasm showed an infiltrating pattern (Figure 8A). Besides, isolated tumor cell nests invaded the gland (Figure 8B). The surgical edges were free of neoplasia. The stroma between the cellular clusters was desmoplastic with frequent plexiform osseous metaplasia (Figure 9A) and occasional calcification or a giant cell granuloma around keratin (Figure 9B). The outer stroma surrounding the neoplasm showed abundant hyalinized, eosinophilic collagen bundles (keloidal collagen) in a haphazard array.

The IHC study revealed strong positivity in the basaloid cells for pan-cytokeratin (pan-CK) AE1/AE3, CK19, high-molecular-weight CK (HMWCK) (Figure 10A), cluster of differentiation (CD)10 (Figure 10B), p63 (Figure 10C), and p40 (Figure 10D), in a diffuse pattern. β-Catenin showed intense nuclear and cytoplasmic expression in the basaloid cells with negativity in the shade (ghost) cells (Figure 11A). Ki67 (MIB-1) was expressed in about 95% of basaloid cells in some ("hot") areas (Figure 11B). Negativity was observed for nuclear protein in testis (NUT), CD117, discovered on gastrointestinal stromal tumor (GIST) 1 (DOG1) [anoctamin 1 (ANO1)], CD99, CD56, CD57, neuron-specific enolase (NSE), chromogranin A, synaptophysin, CD34, calponin, S100, SRY-box transcription factor 10 (SOX10), epithelial membrane antigen (EMA), and alpha-smooth muscle actin (α-SMA). α-SMA revealed abundant myofibroblasts in the intraneoplastic stroma. Parotid tissue showed marked adipose infiltration.

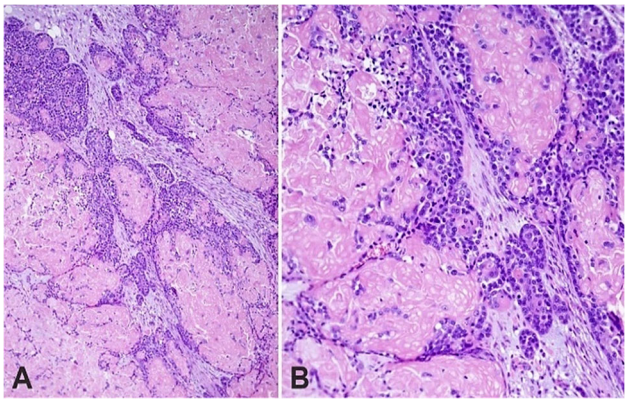


**Figure 4** – ***Basaloid squamous cell carcinoma with shadow (ghost) cell differentiation. Large and small irregularly shape tumor nests: (A) Panoramic view; (B) Medium power image. HE staining: (A) ×100; (B) ×200. HE: Hematoxylin–Eosin.***

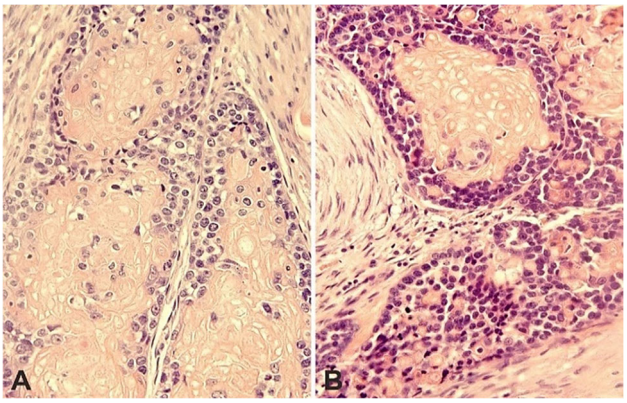


**Figure 5** – ***Basaloid cells nests with prominent shadow (ghost) cell differentiation. Basaloid cells show high nuclear/cytoplasmic ratio: (A) Often the nuclei show one or more nucleoli; (B) Presence of cellular palisades at the edge of the tumor nests. HE staining: (A and B) ×400. HE: Hematoxylin–Eosin.***

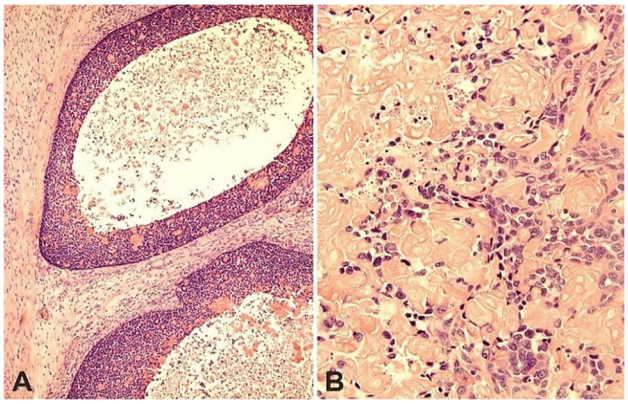


**Figure 6** – ***Large round nests of basaloid cells exhibit comedonecrosis (A) or single-cell necrosis (B). HE staining: (A) ×100; (B) ×400. HE: Hematoxylin–Eosin.***

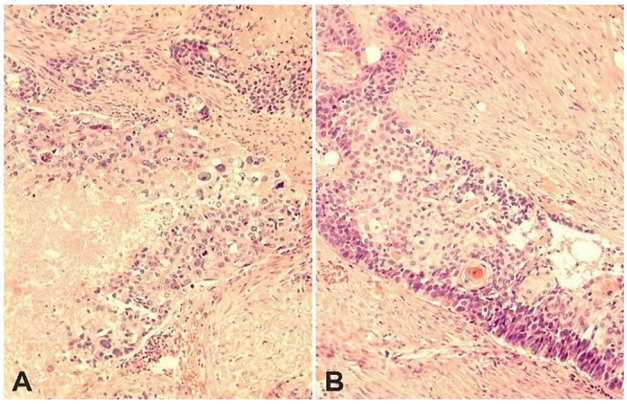


**Figure 7** – ***(A) Basaloid area showing pleomorphism, mitoses, and confluent necrosis; (B) Squamous differentiation focus – a peripheral palisade is evident. HE staining: (A and B) ×200. HE: Hematoxylin–Eosin.***

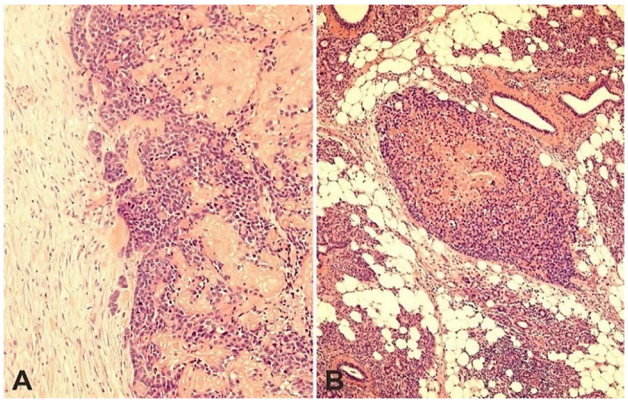


**Figure 8** – ***(A) Infiltrative pattern in the periphery of the tumor; (B) Isolated tumor nest in the glandular tissue. HE staining: (A) ×200; (B) ×100. HE: Hematoxylin–Eosin.***

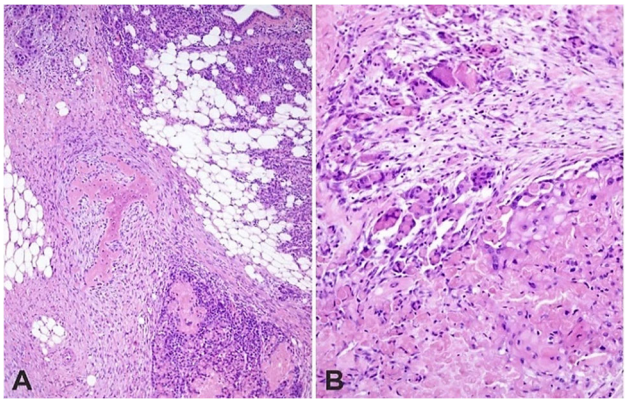


**Figure 9** – ***Reactive changes: (A) Plexiform osseous metaplasia in the stroma; (B) Giant cell granuloma around shadow (ghost) cell differentiation. HE staining: (A) ×100; (B) ×200. HE: Hematoxylin–Eosin.***

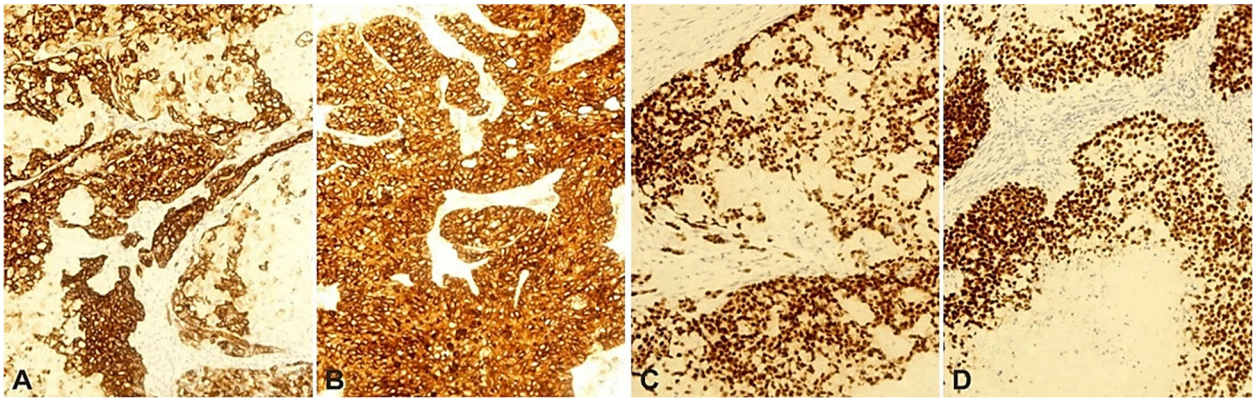


**Figure 10** – ***Immunohistochemistry (×200). The tumor is widely positive for: (A) HMWCK; (B) CD10; (C) p63; (D) p40. CD10: Cluster of differentiation 10; HMWCK: High molecular weight cytokeratin.***

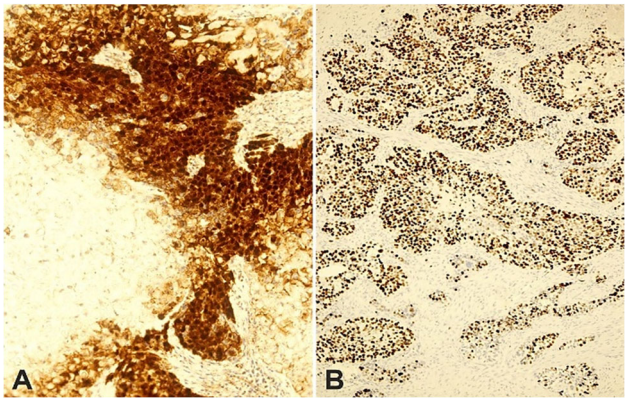


**Figure 11** – ***Immunohistochemistry: (A) Strong nuclear and cytoplasmic positivity for β-catenin (×200); (B) Area with high expression of Ki67 (×100).***

## Discussions

Wain *et al.* established the criteria for the diagnosis of BSCC [1]. BSCC presents a characteristic histopathological biphasic pattern, including small to large size clusters of basaloid cells and conventional squamous components. Basaloid cells have a high nuclear to cytoplasmic ratio and show hyperchromatic nuclei with presence of nucleoli and scant cytoplasm. These cells at the edges of the nests may show peripheral palisading and a thick basement membrane. Abrupt areas of conventional SCC with keratinization in absence of transition cells are usually present, but always constituting a minor component. Pseudoglandular spaces, a cribriform growth pattern, stromal hyalinization, comedonecrosis, high mitotic activity, and apoptosis can be noted in this neoplasm [1, 2]. IHC studies demonstrate strong positivity for HMWCK, p63, and p40, in a diffuse pattern. Our case in addition contained numerous shadow (ghost) cells. In our case, the tumor lacked pseudoglandular spaces or a cribriform growth pattern.

BSCC shows a preferent location for the upper aerodigestive tract [1–4], but can arise in various anatomical sites, including the esophagus [35], anus [36], urinary bladder [37], lung [38], thymus [39], uterine cervix [40], penis [41], and vulva [42]. The tumor rarely affects the parotid gland. Thus, Rivero *et al.* [5] reported the only known case in that location.

Most BSCC patients present with advanced-stage disease. Additionally, BSCC has dual behavior. Disease-specific survival is significantly better in the BSCC group compared to conventional SCC when tumors were located in the oropharynx. In contrast, disease-specific survival is worse for BSCC patients with laryngeal tumors. However, similar disease-specific survival is observed in both tumor types when located in the sinonasal, oral, and hypopharyngeal sites [4].

IHC positive markers like $\beta$-catenin, p40, p63, pan-CK AE1/AE3, CK19, HMWCK (34$\beta$E12), and CD10 are valuable to diagnosis BSCC with SCD and helps to distinguish from other malignancies. As in our case, SOX10 is negative in 41% of BSCCs [43].

BSCC belongs to the group of tumors that present primitive round cells and abrupt keratinization. The differential diagnosis in the parotid gland includes NUT carcinoma (NC), adamantinoma-like Ewing sarcoma (ALES), embryonal carcinoma (EC), and basal cell adenocarcinoma (BCA) of the solid type. NC is an uncommon, highly lethal subtype of SCC defined by translocations involving the *NUT* gene (15q14), most commonly with bromodomain containing 4 (*BRD4*) (19p13). NC typically consists of sheets of monomorphic primitive round cells, with prominent nucleoli, that exhibit focal abrupt squamous differentiation. Immunohistochemically, cells show speckled nuclear positivity for NUT (C52B1 antibody, which shows 100% specificity and 87% sensitivity). Besides, the tumor is frequently positive for pan-CK AE1/AE3, EMA, p63, and p40 [44, 45]. ALES is a rare variant of Ewing sarcoma that is defined by epithelial differentiation, including abrupt keratin pearl formation, and expression of HMWCK, p63, p40, membranous CD99, and NKX2.2 nuclear homeobox protein. The tumor also shows focal positivity for neuroendocrine markers, most commonly synaptophysin. Additionally, ALES harbors a recurrent *t*(11;22) Ewing sarcoma breakpoint region 1–Friend leukemia integration 1 transcription factor (*EWSR1*– FLI1) translocation [46–48]. A unique case of EC was described in a 12-year-old boy. The tumor was composed of solid undifferentiated areas of cells with pale cytoplasm, epidermoid structures with keratinization, and acinic formations. The round-to-oval nuclei of undifferentiated cells showed peripheral heterochromatin or a prominent nucleolus. Transitional cells were not present. The epidermoid cells were reactive for carcinoembryonic antigen and pan-CK AE1/AE3; and the acinic cells for amylase [49]. However, this single-case tumor has not been validated with current IHC techniques. BCA is a low-grade tumor. The solid type is made of basal neoplastic cells forming nest structures that show peripheral palisading. Ducts, mature squamous differentiation with keratin production and pearl formation, and sebaceous elements can be present. Characteristically, BCA is an infiltrating tumor and has a slight potential for metastasis. Perineural invasion is observed in one-third of cases [50]. IHC staining of this neoplasm demonstrates a triphasic profile. Thus, (*i*) the peripheral dark, palisaded cells of the nests are myoepithelial and positive for $\alpha$-SMA, HMWCKs, p63, and p40; (*ii*) the overlying and intermediate pale cells are positive only for HMWCKs, p63, and p40; and (*iii*) when there are ducts, they are strongly positive for CK, and the other cells are weakly positive [50].

Terminal differentiation includes cells that are no longer proliferative and eventually undergo cell death. That term comprises epidermal and trichilemmal keratinization, and SCD [6, 51]. Shadow (ghost) cells are characterized by an ovoid or polyhedral, pale, eosinophilic, well-delimited cytoplasm with a central clear area that replaces the nucleus. They are dying cells with karyolysis and well-preserved cytoplasm [6, 7]. Precursors of shadow (ghost) cells (basaloid cells) show nuclear accumulation of $\beta$-catenin and DNA double-strand breaks (revealed by immunohistochemistry for $\beta$-catenin and single-stranded DNA), and absence of cleaved caspase-3 or cleaved lamin A. This fact suggests that SCD is a caspase-independent programmed cell death and a distinct process from epidermal or trichilemmal keratinization [6]. Nuclear accumulation of $\beta$-catenin consistently suggests catenin beta 1 (*CTNNB1*) gene mutation and activation of the Wnt signaling pathway [51, 52]. According to the classification by Leist & Jäättelä [53], SCD is a type of apoptosis-like programmed cell death.

As previously mentioned, SCD is not restricted to pilomatricoma and other cutaneous tumors with follicular differentiation [7–10], COC [9], DGCT [11], GCOC [12], adamantinomatous craniopharyngioma [9, 13], and gonadal teratomas [14, 15], but has uncommonly been described in visceral carcinomas [16–30]. The locations of these carcinomas include stomach [29], colon [16, 22], rectum [18], uterus [16, 24, 26, 27, 30], ovary [17, 21], urinary bladder [23, 28], gallbladder [19], and lung [20]. These visceral carcinomas correspond to adenoacanthomas, adenosquamous carcinomas, SCCs, or urothelial carcinomas with squamous differentiation [6, 20, 23, 25, 28]. SCD is most commonly seen in

endometrioid adenocarcinomas. Its frequency varies from 15.3% to 24% [26, 27].

SCD has very unusually been described in minor salivary gland tumors (five cases). Eversole *et al.* [31] in a study of 17 cases of mucoepidermoid carcinoma of minor salivary glands commented that one tumor showed keratinized ghost cells admixed with epidermoid cells similar to that observed in pilomatricoma. Schmidt *et al.* [32] reported shadow (ghost) cells in three cases of pleomorphic adenoma, two cases located in the palate, and one case in the lip. Ihrler *et al.* [31] documented one case of the floor of the mouth with prominent SCD and considered it a new entity called salivary ghost cell carcinoma. However, this interpretation has been questioned by other authors [34, 54].

Shadow (ghost) cells are derived from the squamous/squamoid components of the extracutaneous tumors [6, 27] and they are not subjected to degradation even in old lesions. Reactive changes such as giant cell granulomas, calcification, and/or ossification may appear in relation to the SDC.

Recently, Harada *et al.* [34] described a single case of parotid SCC with a prominent shadow (ghost) population. To our knowledge, SCD has not been previously reported in the BSCC of the parotid gland. The case of Harada *et al.* [34] and the present case are the only ones that affect a major salivary gland. Given the history of multiple skin malignant tumors of our patient, possibly he had a genetic predisposition to tumor transformation.

Despite its rarity, BSCC with SCD should be added to the list of primary epithelial tumors of the parotid gland. This special type of keratinization should be recognized to avoid diagnostic errors, especially in small samples. In the reviewed publications, SCD in extracutaneous tumors does not appear to modify tumor behavior. Apparently, the tumor prognosis depends on the basic component and not on the differentiation into shadow (ghost) cells, which is a terminal differentiation.

## Conclusions

We describe for the first time a unique case of parotid BSCC with prominent SCD. Tumor cells showed expression of $\beta$-catenin in nuclei and cytoplasm, suggesting a role of the Wnt signaling pathway in tumorigenesis. SCD is different from apoptosis, epidermal, and trichilemmal keratinization that the inexperienced can interpret as non-descript keratinization. SCD in the tumor does not appear to modify tumor behavior since those cells have a terminal differentiation. The main differential diagnoses of the parotid BSCC with SCD include NC, ALES, EC, and BCA. Although rare, BSCC with SCD should be added to the list of tumors that may originate in the parotid. Knowledge of the morphology of shadow (ghost) cells is essential to recognize this tumor, especially in limited biopsies.

### Conflict of interests

The authors declare that they have no conflict of interests.

### Compliance with ethical standards

No Ethics Committee approval is required in our institution for a case report involving a single patient.

### Consent

Written informed consent was obtained from the patient for publication of this case report and all accompanying images.

### Funding

This study was not funded externally.

## References

[1] Wain SL, Kier R, Vollmer RT, Bossen EH. Basaloid-squamous carcinoma of the tongue, hypopharynx, and larynx: report of 10 cases. Hum Pathol, 1986, 17(11):1158–1166. https://doi.org/10.1016/s0046-8177(86)80422-1 PMID: 3770734

[2] Banks ER, Frierson HF Jr, Mills SE, George E, Zarbo RJ, Swanson PE. Basaloid squamous cell carcinoma of the head and neck. A clinicopathologic and immunohistochemical study of 40 cases. Am J Surg Pathol, 1992, 16(10):939–946. https://doi.org/10.1097/00000478-199210000-00003 PMID: 1384369

[3] Ereño C, Gaafar A, Garmendia M, Etxezarraga C, Bilbao FJ, López JI. Basaloid squamous cell carcinoma of the head and neck: a clinicopathological and follow-up study of 40 cases and review of the literature. Head Neck Pathol, 2008, 2(2):83–91. https://doi.org/10.1007/s12105-008-0045-6 PMID: 20614328 PMCID: PMC2807543

[4] Fritsch VA, Lentsch EJ. Basaloid squamous cell carcinoma of the head and neck: location means everything. J Surg Oncol, 2014, 109(6):616–622. https://doi.org/10.1002/jso.23536 PMID: 24464879

[5] Rivero A, Tang CG, Rasgon BM. Bilateral basaloid squamous cell carcinoma of the parotid gland: a case report and review of the literature. Perm J, 2017, 21:16-042. https://doi.org/10.7812/TPP/16-042 PMID: 28333602 PMCID: PMC5363892

[6] Nakamura T. Shadow cell differentiation: a comparative analysis of modes of cell death with apoptosis and epidermal/trichilemmal keratinization. Dermatopathology (Basel), 2018, 5(3):86–97. https://doi.org/10.1159/000490491 PMID: 30197883 PMCID: PMC6120400

[7] Jacobson M, Ackerman AB. "Shadow" cells as clues to follicular differentiation. Am J Dermatopathol, 1987, 9(1):51–57. https://doi.org/10.1097/00000372-198702000-00011 PMID: 3565713

[8] Ciucă EM, Sălan AI, Camen A, Matei M, Şarlă CG, Mărgăritescu C. A patient with pilomatricoma in the parotid region: case report and review of the literature. Rom J Morphol Embryol, 2018, 59(3):917–926. PMID: 30534834

[9] Hassanein AM, Glanz SM, Kessler HP, Eskin TA, Liu C. $\beta$-Catenin is expressed aberrantly in tumors expressing shadow cells. Pilomatricoma, craniopharyngioma, and calcifying odontogenic cyst. Am J Clin Pathol, 2003, 120(5):732–736. https://doi.org/10.1309/EALE-G7LD-6W71-67PX PMID: 14608900

[10] Hoang MP, Levenson BM. Cystic panfolliculoma. Arch Pathol Lab Med, 2006, 130(3):389–392. https://doi.org/10.5858/2006-130-389-CP PMID: 16519571

[11] Kim SA, Ahn SG, Kim SG, Park JC, Lee SH, Kim J, Yoon JH. Investigation of the beta-catenin gene in a case of dentinogenic ghost cell tumor. Oral Surg Oral Med Oral Pathol Oral Radiol Endod, 2007, 103(1):97–101. https://doi.org/10.1016/j.tripleo.2005.10.037 PMID: 17178501

[12] Qin Y, Lu Y, Zheng L, Liu H. Ghost cell odontogenic carcinoma with suspected cholesterol granuloma of the maxillary sinus in a patient treated with combined modality therapy: a case report and the review of literature. Medicine (Baltimore), 2018, 97(7):e9816. https://doi.org/10.1097/MD.0000000000009816 PMID: 29443742 PMCID: PMC5839843

[13] Buslei R, Nolde M, Hofmann B, Meissner S, Eyupoglu IY, Siebzehnrübl F, Hahnen E, Kreutzer J, Fahlbusch R. Common mutations of beta-catenin in adamantinomatous craniopharyngiomas but not in other tumours originating from the sellar region. Acta Neuropathol, 2005, 109(6):589–597. https://doi.org/10.1007/s00401-005-1004-x PMID: 15891929

[14] Ulbright TM, Srigley JR. Dermoid cyst of the testis: a study of five postpubertal cases, including a pilomatrixoma-like variant, with evidence supporting its separate classification from mature testicular teratoma. Am J Surg Pathol, 2001, 25(6):788–793. https://doi.org/10.1097/00000478-200106000-00011 PMID: 11395557

[15] Zámecnik M, Mukensnábl P, Curík R, Michal M. Shadow cell differentiation in testicular teratomas. A report of two cases. Cesk Patol, 2005, 41(3):102–106. PMID: 16161455
[16] Zámecník M, Michal M. Shadow cell differentiation in tumours of the colon and uterus. Zentralbl Pathol, 1995, 140(6):421–426. PMID: 7538784
[17] Fang J, Keh P, Katz L, Rao MS. Pilomatricoma-like endometrioid adenosquamous carcinoma of the ovary with neuroendocrine differentiation. Gynecol Oncol, 1996, 61(2):291–293. https://doi.org/10.1006/gyno.1996.0142 PMID: 8626150
[18] Nakayama H, Kimura A, Okumichi T, Miyazaki E, Kajihara H, Enzan H. Metaplastic shadow cells in rectal adenocarcinoma: report of a case with immunohistochemical study. Jpn J Clin Oncol, 1997, 27(6):427–432. https://doi.org/10.1093/jjco/27.6.427 PMID: 9438008
[19] Zámecník M, Michal M, Mukensnábl P. Pilomatrixoma-like visceral carcinomas. Histopathology, 1998, 33(4):395. https://doi.org/10.1046/j.1365-2559.1998.00125.x PMID: 9822938
[20] García-Escudero A, Navarro-Bustos G, Jurado-Escámez P, Ríos-Martín J, González-Cámpora R. Primary squamous cell carcinoma of the lung with pilomatricoma-like features. Histopathology, 2002, 40(2):201–202. https://doi.org/10.1046/j.1365-2559.2002.1179b.x PMID: 11952868
[21] Lalich D, Tawfik O, Chapman J, Fraga G. Cutaneous metastasis of ovarian carcinoma with shadow cells mimicking a primary pilomatrical neoplasm. Am J Dermatopathol, 2010, 32(5):500–504. https://doi.org/10.1097/DAD.0b013e3181c6dfc1 PMID: 20526175
[22] Kazakov DV, Spagnolo DV, Kacerovska D, Rychly B, Michal M. Cutaneous type adnexal tumors outside the skin. Am J Dermatopathol, 2011, 33(3):303–315. https://doi.org/10.1097/DAD.0b013e3181db1da3 PMID: 20711062
[23] Nakamura T. Bladder carcinoma with shadow cell differentiation: a case report with immunohistochemical analyses. Int J Clin Exp Pathol, 2012, 5(8):840–844. PMID: 23071867 PMCID: PMC3466982
[24] Squillaci S, Marchione R, Piccolomini M, Chiudinelli M, Fiumanò E, Ungari M. Uterine endometrioid adenocarcinoma with extensive pilomatrixoma-like areas. A case report. Pathologica, 2013, 105(1):8–10. PMID: 23858944
[25] Zamecnik M, Jando D, Kascak P. Ovarian basaloid carcinoma with shadow cell differentiation. Case Rep Pathol, 2014, 2014: 391947. https://doi.org/10.1155/2014/391947 PMID: 24639909 PMCID: PMC3929990
[26] Zámečník M, Bartoš P, Kaščák P. Shadow cell differentiation in endometrioid carcinomas of the uterus. Its frequent occurrence and beta-catenin expression. Cesk Patol, 2015, 51(3):123–126. PMID: 26421953
[27] Nakamura T. Shadow cell differentiation from squamoid morule in endometrial adenoacanthoma. Int J Clin Exp Pathol, 2015, 8(10):13120–13124. PMID: 26722510 PMCID: PMC4680455
[28] Behzatoğlu K. Urothelial carcinoma with shadow cell, lipid cell and sebaceous (skin adnexal) differentiation: clinicopathological and immunohistochemical study of 10 cases. Ann Diagn Pathol, 2015, 19(5):314–319. https://doi.org/10.1016/j.anndiagpath.2015.07.002 PMID: 26235883
[29] Nakamura T. Gastric carcinoma with shadow cell differentiation in metastatic lymph nodes. Hum Pathol Case Rep, 2017, 7:19–22. https://doi.org/10.1016/j.ehpc.2016.03.004 https://www.sciencedirect.com/science/article/pii/S2214330015300742
[30] Weisman P, Park KJ, Xu J. FIGO grade 3 endometrioid adenocarcinomas with diffusely aberrant $\beta$-catenin expression: an aggressive subset resembling cutaneous pilomatrix carcinomas. Int J Gynecol Pathol, 2022, 41(2):126–131. https://doi.org/10.1097/PGP.0000000000000775 PMID: 33811207 PMCID: PMC8484367
[31] Eversole LR, Rovin S, Sabes WR. Mucoepidermoid carcinoma of minor salivary glands: report of 17 cases with follow-up. J Oral Surg, 1972, 30(2):107–112. PMID: 4500489
[32] Schmidt LA, Olsen SH, McHugh JB. Cutaneous adnexal differentiation and stromal metaplasia in palate pleomorphic adenomas: a potential diagnostic pitfall that may be mistaken for malignancy. Am J Surg Pathol, 2010, 34(8):1205–1210. https://doi.org/10.1097/PAS.0b013e3181e658a5 PMID: 20661019
[33] Ihrler S, Mollenhauer M, Weitmayr B, Haas CJ. Salivary ghost cell carcinoma: case report and proposal of a new entity. Virchows Arch, 2020, 476(3):465–468. https://doi.org/10.1007/s00428-019-02657-y PMID: 31616980
[34] Harada H, Sato MP, Otsuki N, Kawamura M, Kurose A, Satou T. A novel parotid carcinoma with a prominent ghost cell population: a masquerading tumor or "salivary ghost cell carcinoma"? Med Mol Morphol, 2022, 55(1):76–83. https://doi.org/10.1007/s00795-021-00302-9 PMID: 34392428
[35] Chen SB, Weng HR, Wang G, Yang JS, Yang WP, Li H, Liu DT, Chen YP. Basaloid squamous cell carcinoma of the esophagus. J Cancer Res Clin Oncol, 2012, 138(7):1165–1171. https://doi.org/10.1007/s00432-012-1180-8 PMID: 22419439
[36] Graham RP, Arnold CA, Naini BV, Lam-Himlin DM. Basaloid squamous cell carcinoma of the anus revisited. Am J Surg Pathol, 2016, 40(3):354–360. https://doi.org/10.1097/PAS.0000000000000594 PMID: 26866355
[37] Vakar-López F, Abrams J. Basaloid squamous cell carcinoma occurring in the urinary bladder. Arch Pathol Lab Med, 2000, 124(3):455–459. https://doi.org/10.5858/2000-124-0455-BSCCOI PMID: 10705407
[38] Yuan G, Zhan C, Huang Y, Zhu D, Xie H, Wei T, Lu T, Wang Q, Yang Y, Zhu Y. Clinical characteristics and prognosis of basaloid squamous cell carcinoma of the lung: a population-based analysis. PeerJ, 2019, 7:e6724. https://doi.org/10.7717/peerj.6724 PMID: 31106047 PMCID: PMC6499056
[39] Phen S, Wang MX, Kelling M, Bhattal GK. Metastatic basaloid squamous cell carcinoma of thymic origin. BMJ Case Rep, 2019, 12(9):e228860. https://doi.org/10.1136/bcr-2018-228860 PMID: 31570341 PMCID: PMC6768391
[40] Kwon YS, Kim YM, Choi GW, Kim YT, Nam JH. Pure basaloid squamous cell carcinoma of the uterine cervix: a case report. J Korean Med Sci, 2009, 24(3):542–545. https://doi.org/10.3346/jkms.2009.24.3.542 PMID: 19543425 PMCID: PMC2698210
[41] Cubilla AL, Lloveras B, Alemany L, Alejo M, Vidal A, Kasamatsu E, Clavero O, Alvarado-Cabrero I, Lynch C, Velasco-Alonso J, Ferrera A, Chaux A, Klaustermeier J, Quint W, de Sanjosé S, Muñoz N, Bosch FX. Basaloid squamous cell carcinoma of the penis with papillary features: a clinicopathologic study of 12 cases. Am J Surg Pathol, 2012, 36(6):869–875. https://doi.org/10.1097/PAS.0b013e318249c6f3 PMID: 22367299
[42] Kurman RJ, Toki T, Schiffman MH. Basaloid and warty carcinomas of the vulva. Distinctive types of squamous cell carcinoma frequently associated with human papillomaviruses. Am J Surg Pathol, 1993, 17(2):133–145. https://doi.org/10.1097/00000478-199302000-00005 PMID: 8380681
[43] Rooper LM, McCuiston AM, Westra WH, Bishop JA. SOX10 immunoexpression in basaloid squamous cell carcinomas: a diagnostic pitfall for ruling out salivary differentiation. Head Neck Pathol, 2019, 13(4):543–547. https://doi.org/10.1007/s12105-018-0990-7 PMID: 30498968 PMCID: PMC6854191
[44] Saik WN, Da Forno P, Thway K, Khurram SA. NUT carcinoma arising from the parotid gland: a case report and review of the literature. Head Neck Pathol, 2021, 15(3):1064–1068. https://doi.org/10.1007/s12105-020-01254-9 PMID: 33351171 PMCID: PMC8384986
[45] Bishop JA, Westra WH. NUT midline carcinomas of the sinonasal tract. Am J Surg Pathol, 2012, 36(8):1216–1221. https://doi.org/10.1097/PAS.0b013e318254ce54 PMID: 22534723 PMCID: PMC4124635
[46] Alnuaim H, Alzahrani M, Ghandurah S, Dababo M. Adamantinoma-like Ewing sarcoma of the parotid gland: report of two cases and review of literature. Cureus, 2020, 12(12):e11870. https://doi.org/10.7759/cureus.11870 PMID: 33409103 PMCID: PMC7781571
[47] Bishop JA, Alaggio R, Zhang L, Seethala RR, Antonescu CR. Adamantinoma-like Ewing family tumors of the head and neck: a pitfall in the differential diagnosis of basaloid and myoepithelial carcinomas. Am J Surg Pathol, 2015, 39(9):1267–1274. https://doi.org/10.1097/PAS.0000000000000460 PMID: 26034869 PMCID: PMC4537687
[48] Rooper LM, Jo VY, Antonescu CR, Nose V, Westra WH, Seethala RR, Bishop JA. Adamantinoma-like Ewing sarcoma of the salivary glands: a newly recognized mimicker of basaloid salivary carcinomas. Am J Surg Pathol, 2019, 43(2):187–194. https://doi.org/10.1097/PAS.0000000000001171 PMID: 30285997 PMCID: PMC8115302
[49] Donath K, Seifert G, Lentrodt J. The embryonal carcinoma of the parotid gland. A rare example of an embryonal tumor. Virchows Arch A Pathol Anat Histopathol, 1984, 403(4):425–440. https://doi.org/10.1007/BF00737291 PMID: 6429943

[50] Seethala RR. Salivary gland tumors: current concepts and controversies. Surg Pathol Clin, 2017, 10(1):155–176. https://doi.org/10.1016/j.path.2016.11.004 PMID: 28153132
[51] Nakamura T. Comparative immunohistochemical analyses on the modes of cell death/keratinization in epidermal cyst, trichilemmal cyst, and pilomatricoma. Am J Dermatopathol, 2011, 33(1):78–83. https://doi.org/10.1097/DAD.0b013e3181e3aec1 PMID: 21048491
[52] Xia J, Urabe K, Moroi Y, Koga T, Duan H, Li Y, Furue M. beta-Catenin mutation and its nuclear localization are confirmed to be frequent causes of Wnt signaling pathway activation in pilomatricomas. J Dermatol Sci, 2006, 41(1):67–75. https://doi.org/10.1016/j.jdermsci.2005.09.005 PMID: 16378715
[53] Leist M, Jäättelä M. Four deaths and a funeral: from caspases to alternative mechanisms. Nat Rev Mol Cell Biol, 2001, 2(8):589–598. https://doi.org/10.1038/35085008 PMID: 11483992
[54] Ide F, Ito Y, Nishimura M, Kikuchi K, Kusama K. Ghost/shadow cell differentiation in salivary gland tumors. Virchows Arch, 2020, 477(4):609–610. https://doi.org/10.1007/s00428-020-02749-0 PMID: 32078042

***Corresponding author***
José-Fernando Val-Bernal, Professor, MD, PhD, Pathology Unit, Department of Medical and Surgical Sciences, University of Cantabria, Avda. Cardenal Herrera Oria s/n, 39011 Santander, Spain; Phone +34 942 315098, Fax +34 942 315952, e-mail: fernando.val@unican.es

*Received: September 17, 2021*

*Accepted: August 3, 2022*